Proceedings of the International Gas Turbine Congress 2003 Tokyo
November 2-7, 2003

IGTC2003Tokyo TS-057

Wake Decay within the Stator Vane in a High-Speed Axial-Flow Compressor

Ryuki NOHARA, Kuniyuki IMANARI, Isao FUJII and Yoshinori OOBA

Ishikawajima-Harima Heavy Industries Co.,Ltd.
229, Tonogaya, Mizuho-machi, Nishitama-gun, Tokyo 190-1297, JAPAN

Phone: +81-42-568-7245, FAX: +81-42-568-7247, E-mail: ryuki_nohara@ihi.co.jp

ABSTRACT

It is known that velocity defects in wakes decay by wake chopping when passing through the subsequent cascade in an axial-flow compressor so that excitation power of forced vibration becomes lower. Consequently, design efforts for this matter tend to be minimized. However, recent compressor loading tends to be higher, and then chopped-wakes are more powerful stimuli. Therefore investigation regarding decay characteristics of chopped wakes is needed to maintain aeromechanical reliability. To investigate behaviors of chopped wakes in a high-speed compressor, rotor wake profiles at inlet and exit plane of stator vane were acquired by hot-film anemometers. Experimental wake decay ratio within stator vane was compared with the prediction by two dimensional model and also unsteady stage CFD. Experimental results suggest that decay of chopped-wakes is essentially three-dimensional phenomenon.

NOMENCLATURE

b, b_0	1/2 wake width, initial 1/2 wake width
D, D_0	relative wake depth, initial relative wake depth
h	stator pitch
L_{in}, L_{exit}	wake length
(s-c)	distance, see Fig.1
U, U_0	free stream velocity, initial free stream velocity
U_{inlet}, U_{exit}	stator inlet and exit velocities
U_{min}	wake center velocity
u	axial velocity components
y	circumferential position
β_{abs}	absolute flow angle
β_{exit}	absolute flow angle at stator exit
β_{rel}	flow angle relative to rotor
β_∞, $\beta_{-\infty}$	downstream, upstream absolute flow angle
θ, θ_0	momentum thickness, initial momentum thickness
$\left(\frac{e}{Uq}\right)$	eddy viscosity
A_{inlet}, A_{exit}	amplitude of first harmonic of wake velocity profile at stator inlet and exit
λ	wake decay ratio

INTRODUCTION

It is well known that forced vibration of blades and vanes in axial-flow compressors due to aerodynamic stimulus bring serious troubles in gas turbine engine operation. So far, engineers have spent enormous time to avoid resonance crossings in Campbell diagrams in design phase.

Manuscript Received on April 14, 2003

Recently, numerical techniques of forced response analysis for blade and vane vibration were developed and used in an actual compressor design process. However, there is a reality that it is impossible to avoid all resonance crossings in recent multi-stage compressors, in which aspect ratios of blades and vanes are an order of unity so that many vibration modes exist within narrow frequency band. The present technology level can provide practically accurate solutions, specially for high-order vibration mode responses in which mechanical damping is negligible, as long as accurate information of aerodynamic excitation force are available. Consequently, we are in a position to identify which resonance crossing points in Campbell diagrams is critical and to be changed. In order to realize this, it is the key issue to predict aerodynamic forcing functions due to wakes and static pressure disturbances accurately in design phase.

Recent advancements in CFD made it possible to predict wake velocity profiles coming from a cascade placed just upstream of the reference blade or vane accurately as well as static pressure disturbances produced by a cascade placed just downstream. In our experience, gust is more important than potential disturbance as aerodynamic stimulus so that we discuss only the former in this study. It is known that velocity defects in wakes decay by wake chopping when passing through the subsequent cascade so that excitation power becomes lower. Resultantly, design efforts for this matter tend to be minimized. But recent design trends in higher aerodynamic loading choice make chopped-wakes more powerful stimuli. Therefore, investigation regarding decay characteristics of chopped wakes is needed to maintain aeromechanical reliability.

Wo (1999) investigated non-chopped rotor wake decay with axial gap experimentally and numerically. Poensgen (1990) reported chopped-wake decay within a stator vane measured by hotwire. These data were measured in low speed compressors. As researches using high-speed compressors, Hathaway (1997) revealed chopped wake behavior within a vane using LDV measurement. Van Zante (1997) presented a two-dimensional model to describe chopped-wake decay behavior within a vane and showed a good agreement between theoretical calculations and experimental data obtained by LDV measurement. However, these validations were limited only at mid-span. It is still unknown whether the above two-dimensional theory can be applicable in generally three-dimensional flow-fields.

To investigate behaviors of chopped wakes in three-dimensional flow-fields of a high-speed compressor, rotor wake profiles at inlet and exit plane of stator vane were acquired by hot-film anemometers. Radial distribution of rotor wake decay ratio within stator vane was compared with the prediction by two-dimensional model and also unsteady stage CFD prediction.

TWO DIMENSIONAL WAKE MODEL

Adamczyk (1996) showed wake stretch model based on inlet and exit velocity triangles and airfoil geometry. The model is written by Eq.(1)-(3). Fig.1 shows definitions of the terms. Angles are positive in the counter-clockwise direction. The wake stretching within stator passage is analogous to the lengthening of a wake segment of constant mass as it passes through a converging channel as shown in Fig.1 The wake length ratio across the channel is given by Eq.(3).

Van Zante (1997) showed two dimensional wake decay model which incorporates the effects of both wake stretching and viscous dissipation. Wake depth, width, and velocity profile model which are written by Eq.(4)-(7). The change in relative wake depth is computed from Eq.(5). The wake width can be computed by Eq.(6) using relative wake depth. The wake velocity profile is computed from Eq.(7).

In this presentation, the eddy viscosity in Eq.(5) was set to 0, because the influence of viscous dissipation is smaller than wake stretching.

The wake decay ratio λ, which is computed by Eq.(8), is defined as the first harmonic of Fourier transformation of wake velocity profile at stator exit divided by the one at stator inlet. The harmonics are based on blade passing frequency. The reason for using first harmonics of the wake velocity profile is that the blade excitation force is almost proportionate to the amplitude of first harmonic.

$$\frac{L_{exit}}{L_{in}} = \frac{\sin(b_{rel} - b_{abs})}{\cos b_{abs}}\bigg|_{inlet} \times\left[1+\frac{2(\bar{s}-c)}{h}\sin(b_{exit})+\left(\frac{(\bar{s}-c)}{h}\right)^2\right]^{\frac{1}{2}} \quad (1)$$

where:

$$\frac{\bar{s}-c}{h} = \frac{\cos b_{rel}}{\sin(b_{rel}-b_{-\infty})}\left(\frac{\cos b_{-\infty}}{\cos b_{\infty}}\right) - \frac{4(\tan b_{-\infty}-\tan b_{\infty})}{(\cos b_{-\infty}+\cos b_{\infty})^2}\cos b_{\infty}(\cos b_{-\infty})^2 \quad (2)$$

$$\frac{L_{exit}}{L_{in}} = \frac{U_{exit}}{U_{inlet}} \quad (3)$$

$$D = \frac{U-U_{\min}}{U} \quad (4)$$

$$\frac{D_0}{D} = \left(\frac{U_0}{U}\right)^2\left[1+\frac{8p^2}{p^2-4}\left(\frac{e}{Uq}\right)\int_{x_0}\frac{U_0}{U}d\left(\frac{D_0^2 x}{q_0}\right)\right]^{-\frac{1}{2}} \quad (5)$$

$$\frac{b}{b_0} = \left(\frac{U_0}{U}\right)^3 \frac{\left(\frac{1}{D_0}-\frac{3}{4}\right)}{\left(\frac{1}{D_0}-\frac{3}{4}\frac{D}{D_0}\right)\frac{D}{D_0}} \quad (6)$$

$$\frac{U-u}{U} = D\frac{1}{2}\left[1+\cos\left(p\frac{y}{b}\right)\right] \quad (7)$$

$$l = \frac{A_{exit}}{A_{inlet}} \quad (8)$$

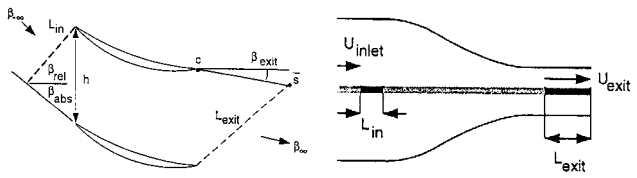

Fig.1 Definition of angles and lengths used in the wake stretching in a 2D converging channel. [Van Zante, 1997]

THREE DIMENSIONAL NUMERICAL SIMULATIONS

Behavior of chopped-wake decay was predicted using unsteady stage numerical simulation which was developed by Hirai et al. (1997). The governing equations are the time-dependent three-dimensional Reynolds-averaged Navier-Stokes equations. The turbulent viscosity is determined by the two-layer Baldwin-Lomax (1978) algebraic turbulence model. An implicit finite difference scheme developed by Chakravarthy and Osher (1985) and central differencing is used for the diffusion terms. Further details on the implicit scheme can be found in Matsuo (1991). For the implicit time integration approach, a Newton sub-iteration is performed at each time step to increase stability and reduce linearization errors. For all cases investigated in this simulation, four Newton sub-iterations were performed at each time step.

The actual compressor had 23 blades and 40 stators, however, blade counts were changed to 24 blades and 48 stators which were retained the original solidity of each airfoil because of calculation speed. In this calculation, all computational domains contained one rotor passage and two stator passages. An H-type grid was used for each blade passage. Grid points for each airfoil passage contained 119x61x71 (streamwise x tangential x radial). Grid points for tip clearance of rotor contained 10 grids. The grids for individual passage overlap by one-mesh in the axial direction. The value of y+ on blade surface is about 30. Fig.2 shows the numerical grid at 60% span. Fig.3 shows one of the results of calculation, which is a contour of entropy at 60% span. Radial distribution of wake decay ratio within stator vane was calculated using predicted unsteady flow velocity.

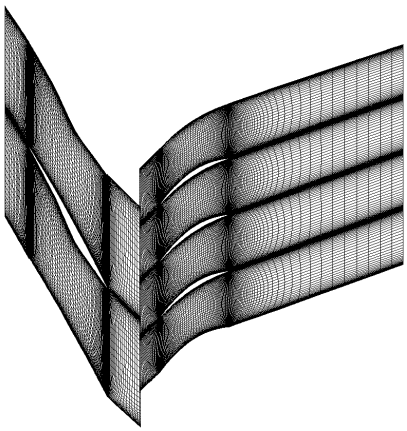

Fig.2 Computational grid

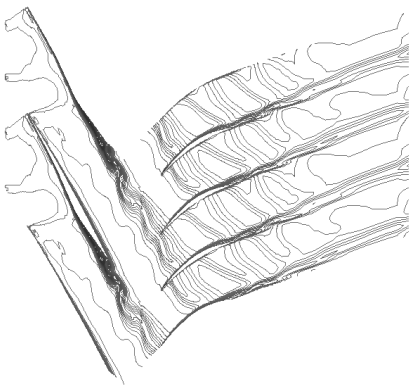

Fig.3 Contour of entropy

TEST COMPRESSOR

The measurements were acquired on in-house single stage compressor which was typical first stage of modern multi-stage compressor. Fig.4 shows the cross section of test compressor rig. Diameter of the rotor blade is about 900mm. Blade height is about 200mm. Blade chord length at mid span is about 100mm. Table 1 shows the specification of test compressor. Fig.5 shows the overall performance map of the compressor at design and 80% speeds.

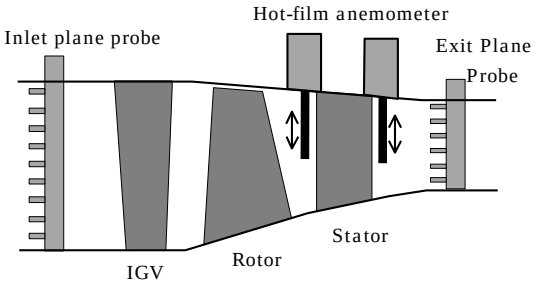

Fig.4 Cross section of test compressor

Table 1 Specification of test compressor

Number of Stage	1
Rotor tip solidity	1.4
Stator tip solidity	1.3
Relative mach number at rotor tip	1.6
Absolute mach number at stator tip	0.6

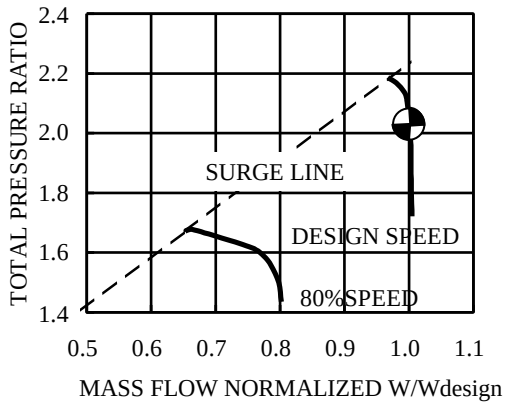

Fig.5 Overall performance of test compressor

INSTRUMENTATION

Overall performance was acquired using total pressure/total temperature combination probes that were located upstream and down stream of the test compressor. Total pressure and absolute flow angle at stator inlet and exit plane were measured by a 5-hole yaw meter that was traversed spanwisely. And total temperature at stator inlet was also measured by calibrated thermocouple probe.

Decay of rotor wakes within stator vane was measured using X-type hot-film anemometer probes (DANTEC model 55R52), which were inserted into position of 5% chord length upstream from stator vane leading edge and 5% chord length downstream from stator vane trailing edge. The probes were inserted into mid-pitch circumferential position of stator vane airfoil to suppressed influences from stator wake and stator potential field. The probe had two quartz fibers located each other at 90 degree angle. And nickel film sensors (70μm x 1.25mm) were vaporized on the fibers. It was installed in the support whose diameter was 6mm. As it was relatively small to the flow field, flow disturbance developed by the probe could be negligible. The support with probe was traversed in span direction by remote controller. Measurement was triggered by pulse signal of rotor shaft. Acquired data was amplified with DANTEC model 90C10 and converted to digital data using A/D converter.

DATA AQUISITION

Before hot-film measurement, steady state total pressure, total temperature, and flow angle data were measured using five-hole yaw meter and thermocouple probe. Afterwards unsteady flow velocities were measured by hot-film probe at the same measuring locations. The probe angle was set according to the flow angle which was measured by the yaw-meter.

Data sampling frequency was set to about 45 times of blade passing frequency at design speed, and 2048 data was acquired in one sequential measurement. One sequential data at design speed contained about two cycles of rotor revolution data. After the measurement was repeated 512 times at each span location, ensemble average of these data was calculated to remove the influence of fluctuation of wake profile. At design speed and 80% speed condition, rotor wake profiles were acquired at 80,70,60, and 50% span from hub using the above-mentioned process.

RESULTS AND DISCUSSION

Relative velocity of rotor was calculated from acquired data and wake profiles of each blade were obtained. To remove each individual difference of wake profiles, Wake profiles of each blade were averaged.

Fig.6 shows measured wake velocity profiles near 60% span at just upstream and just downstream of stator vane at design speed. Fig.7 shows the harmonics of Fourier transformation of wake velocity at inlet and exit of stator vane in design speed. Fig.8 and Fig.9 show the wake profiles and harmonics near 60% span in 80% speed.

Fig.10 shows the radial distribution of wake decay ratio at design and 80% rotation speeds. Wake decay ratio was defined as the amplitude of first harmonic at stator exit divided by the one at stator inlet.

We can see that there is a considerable change in wake decay ratio in the radial direction. The trend is similar for both of design and 80% rotation speeds.

In CFD results, wake decay ratio near 60% span met maximum at design speed. The radial profile of wake decay ratio predicted by CFD is similar to test result at design speed. CFD results can reproduce the radial profile of experimental results fairly well with the exception of the location of maximum wake decay ratio.

The predicted radial distribution of wake decay ratio by the two-dimensional model, which was computed by Eq.(1)-(8), was compared with experiment in Fig.10. It is found that there is an apparent difference between two-dimensional theory and experiment. This fact suggests that decay of chopped-wakes is essentially three-dimensional phenomenon.

As a reason of similar radial profiles in wake decay ratio between test results and CFD results, the rotor wake drift in radial direction within stator vane is speculated. The radial velocity in rotor wake field is different from the one in main flow field at stator inlet. This can produce wake drifts.

CONCLUSION

To investigate behavior of chopped-wake decay, experimental data by hot-film anemometer was acquired. The radial distribution of wake decay ratio was compared with prediction by 2D model and 3D unsteady CFD prediction. As a result, experimental radial distribution of rotor wake decay ratio does not agree to the prediction by two dimensional wake decay model. Therefore, three-dimensional influences of wake decay should be needed to consider to explain behavior of chopped wake.

Three-dimensional unsteady CFD could predict the feature of rotor wake decay ratio.

Finding out the detailed reason of changing of wake decay ratio in radial direction, which is unexplained by 2D model, will be next assignment.

REFERENNCES

John J.Adamczyk, "Wake Mixing In Axial Flow Compressors", ASME Paper No.96-GT-29, 1996

A.M.WO, M.H.Chung, S.J.Chang, S.F.Lee, "Wake Vorticity Decay and Blade Response in an Axial Compressor", ASME Paper No.99-GT-451,1999.

Poensgen, H.E.Gallus, "Three-Dimensional Wake Decay Inside of a Compressor Cascade and Its Influence on the Downstream Unsteady Flow Field Part I : Wake Decay Characteristics in the Flow Passage",ASME Paper No.90-GT-21,1990

M.D.Hathaway, T.H.Okiishi, K.L.Suder, A.J.Strazisar, J.J.Adamczyk, "Measurements of the unsteady Flow Field Within the Stator Row of a Transonic Axial-Flow Fan I - Measurement and Analysis Technique", ASME Paper No.87-GT-226,1997

Dale E.Van Zante, Jhon J.Adamczyk, Anthony J.Strazisar, Theodore H.Okiishi, "WAKE RECOVERY PERFORMANCE BENEFIT IN A HIGH-SPEED AXIAL COMPRESSOR", ASME Paper No.97-GT-535,1997

K.Hirai and H.Kodama, O.Nozaki, K.Kikuchi, A.Tamura and Y.Matsuo, "Unsteady Three-Dimensional Analysis of Inlet Distortion In Turbomachinery", AIAA-97-2735, 1997

Baldwin, B.S., and Lomax, H., "Thin-Layer Approximation and Algebraic Model for Separated Turbulent Flows", AIAA-78-257, 1978

Chakravarthy,S.R. and Osher,S., "A New Class of High Accuracy TVD Schemes for Hyperbolic Conservation Laws", AIAA-85-0363, 1985

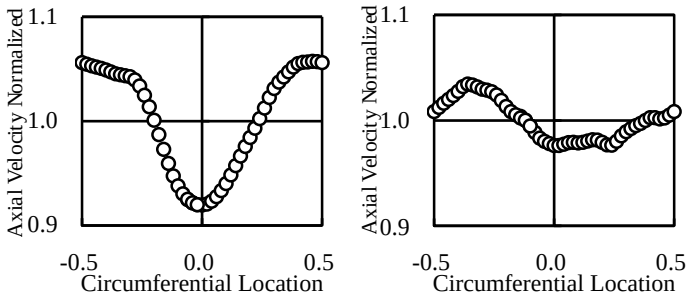

Fig.6 Wake profile at 60% span at design speed

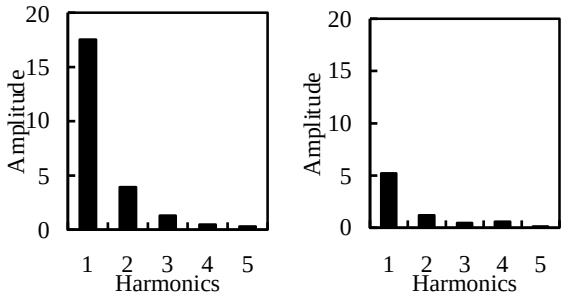

Fig.7 Fourier transformation at design speed

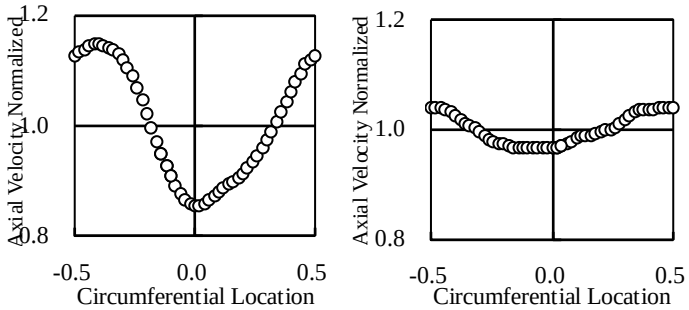

Fig.8 Wake profile at 60% span at 80% speed

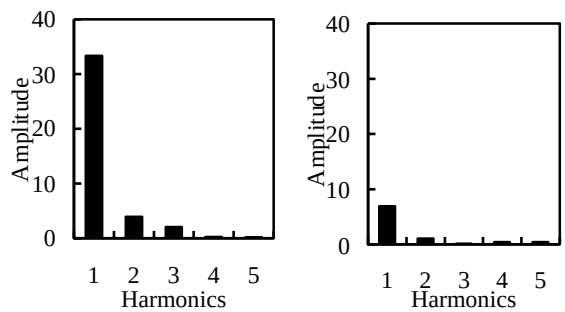

Fig.9 Fourier transformation at 80% speed

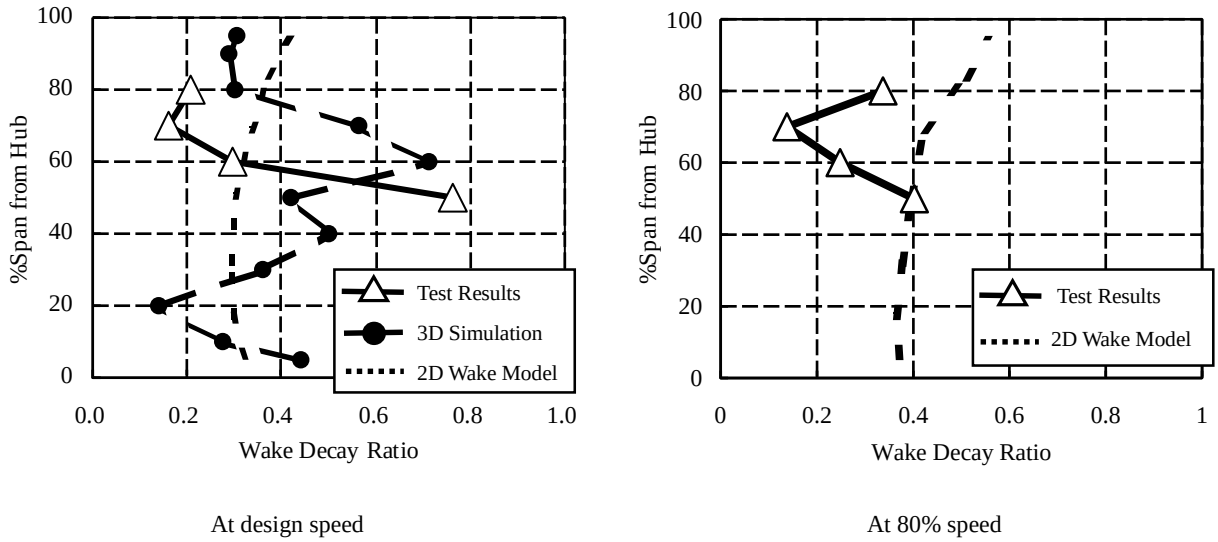

Fig.10 Radial distribution of wake decay ratio